PHOTONIC SENSORS / Vol. 16, No. 1, 2026: 9560006

Applications of uDAS in Exploration and Development of Oil and Gas

Yanbo XIAO[1,2,3], Shujie AN[1,2,3], Yunfei CHEN[1,2], Qiaoling CHEN[1,2], Haifeng CHEN[1,2], Yuntong ZHANG[3], Yuqi WANG[1,2], Wei ZHOU[3], Yu WANG[3], Fengyu TAN[3], Zhihao HE[3], Qinze LI[3], Yuanzhong CHEN[3], Junjun WU[3], Shujun XIA[3], Renzhi ZHANG[3], Ximing WANG[3], Zengling RAN[1,2,3*], and Yunjiang RAO[1,2,3*]

[1]*Key Laboratory of Optical Fiber Sensing & Communications (Ministry of Education of the People's Republic of China), University of Electronic Science and Technology of China, Chengdu 611731, China*

[2]*School of Information and Communication Engineering, University of Electronic Science and Technology of China, Chengdu 611731, China*

[3]*Optical Science & Technology (Chengdu) Co., Ltd., Chengdu 611731, China*

[*]Corresponding authors: Zengling RAN and Yunjiang RAO E-mails: ranzl@uestc.edu.cn and yjrao@uestc.edu.cn

Abstract: In recent years, the fiber-optic distributed acoustic sensing (DAS) technology has played an important role in the oil and gas exploration and development. We develop an industrialized ultra-sensitive DAS instrument, named uDAS, which has world-class performances and robust engineering capability. The uDAS achieves the pε/√Hz level strain resolution and broadband frequency response from millihertz (mHz) to 10 kHz. The uDAS system has been widely applied to onshore and offshore vertical seismic profiling (VSP), hydraulic-fracturing monitoring, surface seismic exploration, near-surface structural investigation, and DAS-uphole, with deployments spanning all oilfields of China National Petroleum Corporation (CNPC), and part oilfields of Saudi Aramco and Abu Dhabi National Oil Company (ADNOC). In this paper, we introduce the key technologies of uDAS and its typical applications over the years. These applications demonstrate the uDAS's ultrahigh sensitivity, broadband frequency response, and high fidelity, enabling near-wellbore fine imaging, high-resolution visualization of downhole fracturing processes, and production optimization. The uDAS is becoming the new generation of all-optical geophones to replace the conventional electronic geophone arrays.

Keywords: Optical fiber sensing; distributed acoustic sensing; exploration and development of oil and gas

Citation: Yanbo XIAO, Shujie AN, Yunfei CHEN, Qiaoling CHEN, Haifeng CHEN, Yuntong ZHANG, *et al*., "Applications of uDAS in Exploration and Development of Oil and Gas," *Photonic Sensors*, 2026, 16(1): 9560006.

1. Introduction

Acoustic sensing is a fundamental technology for signal acquisition and recognition in modern industry and life [1–3]. Among these approaches, fiber-optic distributed acoustic sensing (DAS) enables continuous acquisition of vibration and seismic signals along optical fibers, offering the

Received: 21 October 2025 / Revised: 17 November 2025

DOI: 10.26599/PhoS.2026.9560006
Article type: Review

long sensing range, high sensitivity, dense spatial sampling, and excellent tolerance to harsh environments [4–6]. The DAS has been widely used for hydrophones [7, 8], structural health monitoring [9–11], natural earthquake monitoring [12–14], and perimeter security [15, 16], especially for oil and gas exploration and development [17–21]. In oil and gas industry, the DAS attributes are highly compatible with the sensing requirements across almost all stages [22]. During the exploration stage, the DAS provides the capability for single-run vertical seismic profiling (VSP) [23–25] along entire wellbores and has the ability to replace the conventional electronic geophone arrays, particularly under high-temperature and high-pressure downhole conditions where the traditional geophones suffer from limited sensor capacity, complex field deployment, and poor long-term reliability [26–28]. During the development and production stages, leveraging its spatio-temporal continuity, the DAS has been widely applied for shale-gas and shale-oil hydraulic-fracturing monitoring and fracture propagation analysis [29, 30], providing real-time information to optimize the fracturing process and improve the production efficiency. Meanwhile, its application scope has been expanded to fluid-production profiling [31], long-term reservoir monitoring [32], and underground gas-storage integrity assessment [33]. At present, the primary manufacturers of industrialized DAS instruments include Silixa (the United Kingdom), Halliburton (the United States), Schlumberger (the United States), and Optical Science & Technology (Chengdu) Co., Ltd. (China), etc., worldwide [34–37].

As the application potential of the DAS in oil and gas exploration and development continues to be explored, its performance requirements are becoming increasingly well-defined. When the exploration extends from shallow to deep and ultra-deep reservoirs, DAS systems must achieve the lower noise floor level to acquire the high signal-to-noise-ratio (SNR) seismic data from deep well sections. During the development and production stages, downhole dynamic activities require DAS systems to provide a broadband frequency response from millihertz (mHz) to kHz, enabling detection of ultra-low frequency formation deformation [38] as well as high-frequency transient events, such as sand production or fluid influx [31].

To meet these multi-scenario monitoring requirements, we have developed an ultra-sensitive DAS (uDAS) instrument based on the coherent heterodyne detection architecture [39] that integrates low-noise optical fiber amplification [40] and multi-frequency pulses modulation [41], achieving an ultra-low noise floor and broadband frequency response. To date, the uDAS instrument has been deployed in more than 600 wells, covering almost all the aspects of oil and gas exploration and development, and demonstrating the strong versatility and great potential for wide applications in the VSP, hydraulic-fracturing monitoring, surface seismic exploration, and near-surface structural imaging.

2. uDAS

The most important technology of the uDAS instrument is the heterodyne coherent detection [39], as shown in Fig. 1. Based on this foundation, low-noise optical amplification [40] is integrated to suppress EDFA-generated amplified spontaneous emission (ASE) and enable low-noise amplification of weak Rayleigh backscattered signals. Multi-frequency pulse modulation [41] is also used to statistically mitigate random phase and polarization fading. Therefore, the uDAS instrument achieves the ultra-high SNR, ultra-low noise, ultra-wide bandwidth, and ultra-high spatial resolution.

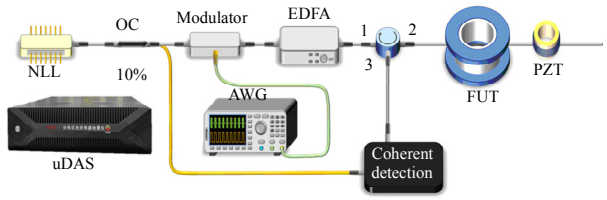

Fig. 1 Schematic diagram of uDAS (NLL: narrow linewidth laser; OC: optical coupler; EDFA: erbium-doped fiber amplifier; AWG: arbitrary waveform generator; FUT: fiber under test; PZT: piezoelectric transducer).

The performances of the uDAS system are characterized by applying vibrational signals to the fiber using a PZT. Figure 2 presents its main performance parameters and response features. In the noise-floor test, we use a 10 km fiber and evaluate the noise floor at the fiber end. As shown in Fig. 2(a), the system exhibits a phase noise floor of approximately −80 dB rad^2/Hz over the 1 Hz–500 Hz range, corresponding to the strain resolution of 2 pε/√Hz with the 5 m gauge length (GL). Figures 2(b)–2(e) illustrate the system's recovery of sinusoidal vibration signals from 0.1 mHz to 10 kHz. Figure 2(f) further shows the response linearity, with an R^2 of 0.999 94, obtained by gradually increasing the PZT driving voltage at 100 Hz. These tests demonstrate that the uDAS features an ultra-low noise floor, broadband response, and high linearity, which offers the ability for the detection of the extremely weak signals and broadband frequency response from mHz to 10 kHz for the oil and gas exploration and development. To position our system, we compare the key performance metrics of the uDAS system with existing industrialized DAS systems in Table 1. The data listed in Table 1 are obtained from the respective companies' websites [42–44].

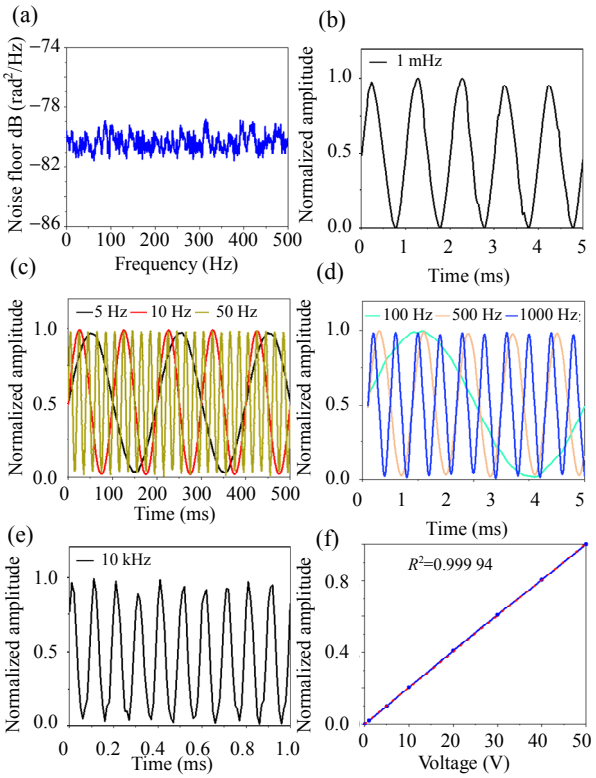

Fig. 2 uDAS performances: (a) noise floor, (b), (c), (d), and (e) vibration signals recovered, and (f) response linearity.

Table 1 Comparison of different DASs.

	uDAS	iDAS of Silixa [42]	DataSphere DAS of Halliburton [43]	Optiq of Schlumberger [44]
Strain resolution	2 pε/√Hz (GL=5 m and length=10 km)	2 pε/√Hz (GL=10 m and length=400 m)	3 pε/√Hz (GL=10 m and length=10 km)	1.5 pε/√Hz (GL=6.4 m and length=5 km)
Gauge length	2 m–40 m	10 m	2 m–40 m	6.4 m
Bandwidth	1 mHz–10 kHz	1 mHz–50 kHz	/	/
Sensing range	80 km	45 km	150 km	50 km

3. Applications

With its pε/√Hz level strain sensitivity and broadband response, the uDAS has been successfully deployed in the DAS-VSP under both onshore and offshore conditions, single-well and offset-well hydraulic-fracturing monitoring, surface seismic exploration, near-surface structural investigations, and DAS-uphole.

3.1 Onshore DAS-VSP

The VSP is an important technology of active

seismic exploration, which can be carried out using either the DAS technology or conventional electronic geophone arrays. Geophones record VSP data at discrete depths, necessitating repeated repositioning and hence limiting their applications in producing wells. In contrast, the uDAS provides a significant improvement in downhole seismic acquisition, enabling continuous and high-density VSP acquisition along the entire wellbore, even in producing wells. The typical configuration of a DAS-based VSP is illustrated in Fig. 3(a), where an active seismic source is activated at the surface, and the uDAS records the propagating seismic wavefields downhole. By tracking the arrival time of the downgoing wavefields, the vertical P-wave velocity is accurately derived. The velocities obtained from the VSP data can further be used to characterize the subsurface composition and monitor fluid migration and reservoir dynamics at the reservoir scale.

A zero-offset VSP survey is conducted using the uDAS in parallel with the conventional electronic geophones within the same borehole, reaching a depth of approximately 4 500 m. Figure 3(b) presents the spliced display of the geophone *Z*-component record (left of the red dotted line) and the uDAS record (right of the red dotted line), exhibiting a high degree of consistency on downgoing and upgoing wavefields between the two datasets. Furthermore, we compute the mean cross-correlation time lag between the geophone and DAS-VSP traces at the same depth points [the 60 channels around the red line in Fig. 3(b)]. The average lag is approximately 1 ms, which is within one sampling interval, as shown in Fig. 3(c). This indicates that the uDAS records meet the requirements for seismic data processing. Figures 4(a) and 4(b) show the complete VSP records acquired by both systems, where the uDAS record demonstrates clear and continuous first-arrival in downgoing waves, as well as clearly identifiable upgoing reflections. Amplitude-spectrum analysis [Figs. 4(c) and 4(d)] indicates that both systems share a comparable effective bandwidth of approximately 5 Hz–90 Hz. The average and interval velocities derived from the two records are displayed in Figs. 4(e) and 4(f), respectively. The average velocities obtained by the uDAS and geophones are nearly identical, while the interval velocity profile from the uDAS reveals finer stratigraphic details, delineating sub-layer variations that enhance fine-scale geological interpretation. So, the uDAS can provide efficient, high-sensitivity, and high-fidelity seismic acquisition, and its high-quality data make it feasible to achieve high-resolution near-wellbore imaging for guiding precise placement of reservoirs.

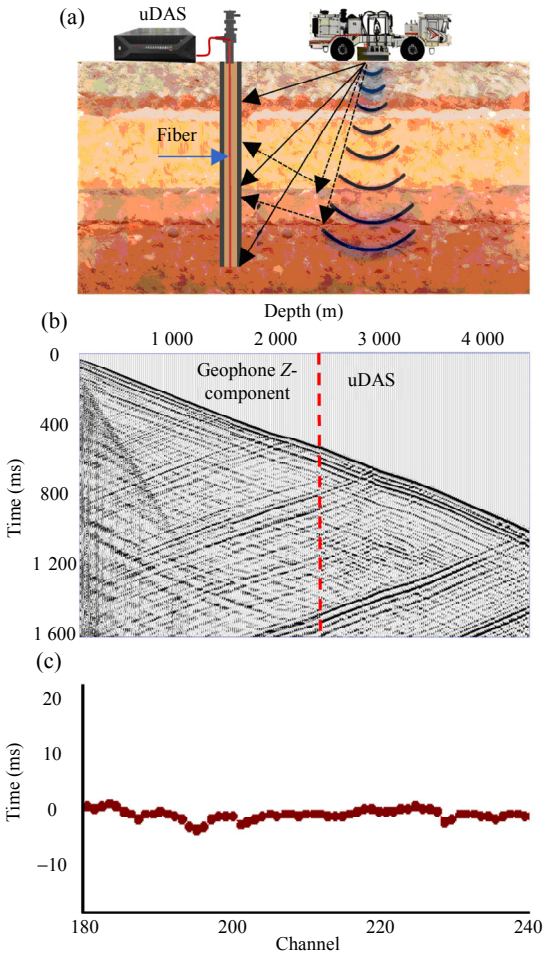

Fig. 3 Schematic diagram and results of the uDAS VSP: (a) acquiring a VSP survey using a uDAS, (b) the spliced display of the geophone *Z*-component record and DAS record, and (c) the cross-correlation time lag between the geophone and uDAS VSP records.

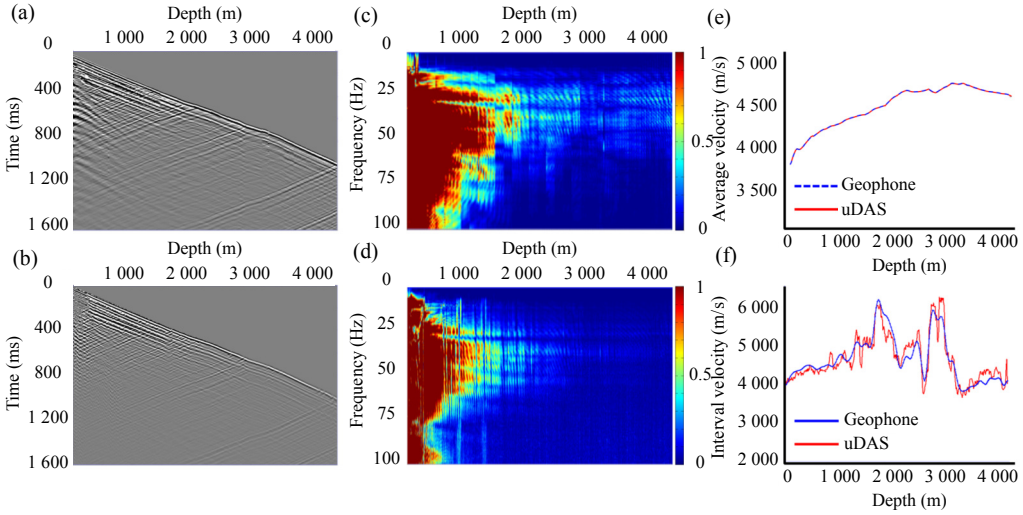

Fig. 4 Comparison of VSP records from geophones and uDAS: (a) geophone VSP record, (b) uDAS VSP record, (c) frequency spectrum of geophone data, (d) frequency spectrum of uDAS data, (e) average velocity comparison, and (f) interval velocity comparison.

3.2 Offshore VSP

Compared with onshore operations, offshore VSP acquisition poses greater technical and operational challenges due to limited well accessibility, complex coupling conditions, and high redeployment costs. The DAS offers a practical and efficient alternative. An offshore VSP survey is conducted using the uDAS with an airgun source to evaluate its field performance. Figure 5(a) shows the DAS-VSP seismic record at an offset of 785 m, exhibiting clear and stable first-arrival with the excellent borehole coupling stability and high sensitivity across the entire well. Figure 5(b) presents the amplitude spectra of raw waveforms extracted from shallow (500 m), intermediate (2 000 m), and deep (3 200 m) intervals, respectively. The spectral responses reveal a stable dominant frequency of approximately 30 Hz across all depths, while the effective bandwidth gradually narrows with depth, from 3 Hz–110 Hz at 500 m to 3 Hz–78 Hz at 3 200 m at −30 dB. This trend reflects the natural attenuation of high-frequency components with depth and confirms that the uDAS maintains a broad and uniform frequency response throughout the entire acquisition range. Notably, the deep section retains the usable high-frequency component up to ~80 Hz, which benefits high-resolution imaging of deep targets.

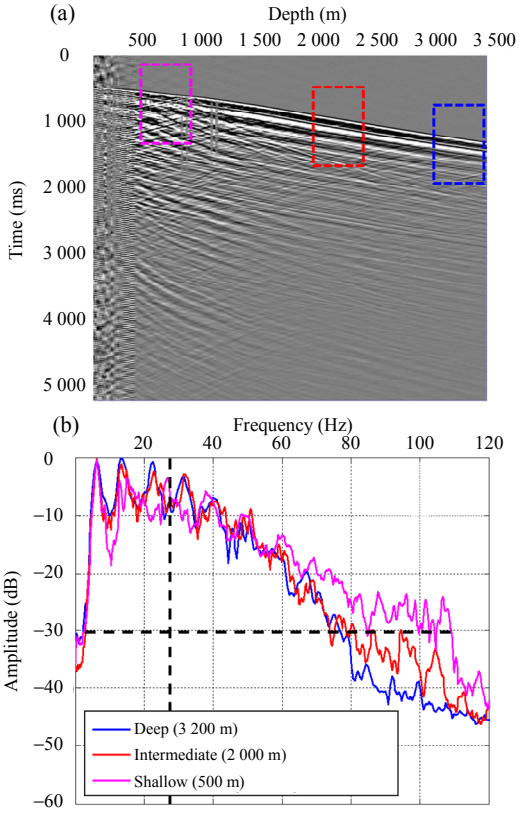

Fig. 5 Results of offshore DAS VSP: (a) offshore DAS VSP record and (b) frequency spectra of seismic signals at shallow, intermediate, and deep zones.

In the same operational area, Ocean Bottom Cable (OBC) and Ocean Bottom Node (OBN) surveys are also conducted. The data from OBC, OBN, and uDAS-VSP are processed, and the resulting stratum images from all three technologies are shown in Fig. 6. Compared with OBC and OBN, the uDAS 3D-VSP delivers the higher resolution in the shallow section (2 000 m–2 400 m), resolving more thin-bed detail vertically, and the lateral amplitude variations along coherent reflectors are more consistent with the geological characteristics of deltaic depositional facies. In the deeper interval (3 100 m–3 600 m), the uDAS-VSP preserves the broader seismic bandwidth, yielding the higher imaging quality and improving the identification of the subtle reservoir.

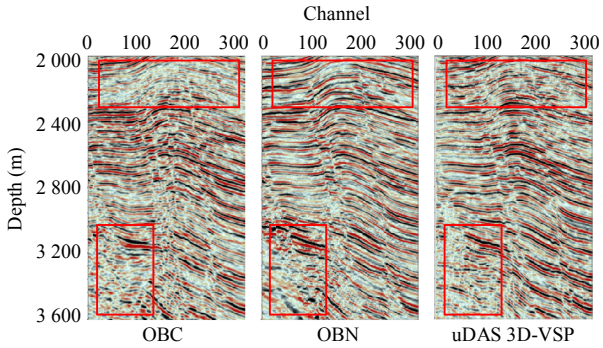

Fig. 6 Structural-imaging comparison: depth sections from OBC, OBN, and uDAS 3D-VSP (the channel spacing is 12.5 m).

3.3 Single-well hydraulic fracturing monitoring

Hydraulic fracturing is the important step in developing shale oil/gas and coalbed methane, wherein high-pressure fluids are injected into tight reservoirs to create or extend fractures and thereby improve hydrocarbon recovery, as shown in Fig. 7. The uDAS can provide an efficient and practical monitoring solution, enabling high-spatial-resolution, high-sensitivity, broadband, and real-time seismic measurements along entire wellbore, and visualizing fracture propagation, fluid transport/placement, and flowback.

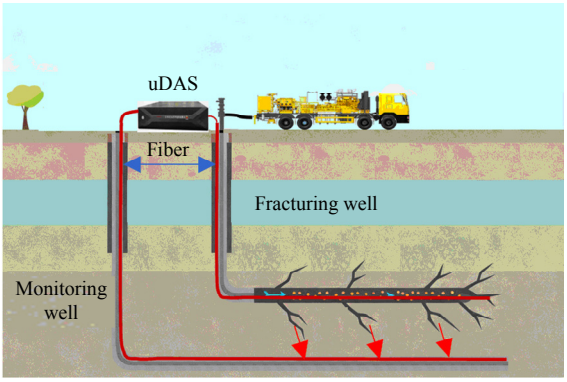

Fig. 7 Schematic diagram of single-well and offset-well hydraulic fracturing monitoring.

The single-well fracturing monitoring operation is conducted using the uDAS. For a representative fracturing stage, the uDAS waterfall plot reveals strong fluid entry near Cluster 2, accompanied by vertically continuous high-energy bands extending into adjacent layers, as shown in Fig. 8(a). This pattern indicates the potential fracture-height growth beyond the designed target interval and reflects the effective proppant transport within the stimulated zone. During the flowback, the uDAS response clearly distinguishes the contributions of each stage to the total production volume. The left part of Fig. 8(b) shows the uDAS waterfall plot during the flowback process. Over the entire monitoring period, we integrate the uDAS response energy at different depths and then calculate the corresponding energy fractions for each depth interval, as shown in the right part of Fig. 8(b). Stage 5 dominates the total flowback with 84.34%, followed by Stages 4 (7.94%) and 6 (5.78%), whereas Stages 1 to 3 exhibit negligible activity, as shown in Fig. 8(b). Such differentiation indicates that the uDAS enables accurate detection of sand and fluid entry, thereby achieving the comprehensive visualization of downhole operations throughout hydraulic fracturing processes.

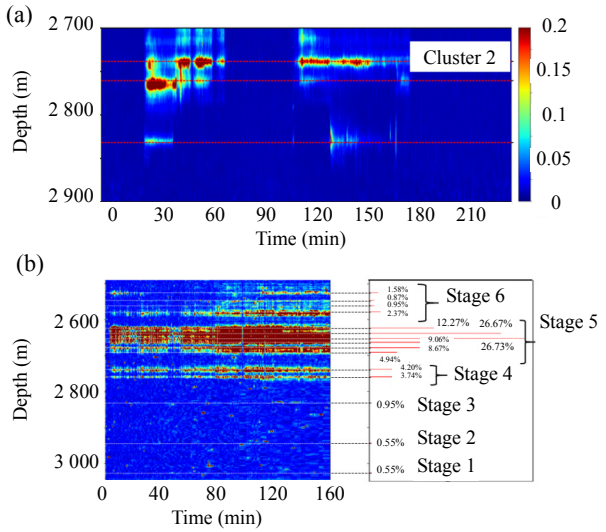

Fig. 8 uDAS time-depth waterfalls: (a) perforation and pumping responses during the fracturing and (b) dynamic response during the flowback.

3.4 Offset-well hydraulic fracturing monitoring

In hydraulic-fracturing operations, the fracture initiation, propagation direction, height, and interwell/interlayer connectivity are critical for evaluating stimulation effectiveness. Real-time observation through the strain responses of neighboring wells is an effective means to identify whether fractures extend to neighboring wells and extra-layer flow occurs to guide on-site adjustment. So, a reliable monitoring system is needed to deliver continuous and distributed coverage along the entire wellbore with meter-scale spatial sampling, and capture ultralow-frequency responses with the high strain resolution. The uDAS is well suited to these requirements.

To monitor formation deformation and evaluate the effectiveness of hydraulic stimulation, an offset-well fracturing monitoring operation is conducted using the uDAS, as shown in Fig. 7. In the field test, the uDAS is deployed in a monitoring well to record formation strain and track fracture evolution. In a typical operation, the complete hydraulic fracturing process lasts for several days, during which the uDAS continuously acquires strain near the monitoring well. We therefore present a representative segment of the monitoring results for illustration. As shown in Fig. 9(a), the uDAS successfully detects fine strain-rate variations below 10^{-3} με/s over 11 hours, clearly revealing the initiation and propagation of fractures. These strain changes exhibit a strong correlation with the casing-pressure fluctuations [Fig. 9(b)] in the fracturing well, confirming that the uDAS can precisely capture the spatial and temporal evolution of the fracture network. The results demonstrate that the uDAS offers the strong capability for long-term monitoring of ultra-low-frequency deformation in complex subsurface environments and provides reliable deformation data for optimizing fracturing strategies (e.g., stage spacing, cluster efficiency, and pump-schedule adjustments).

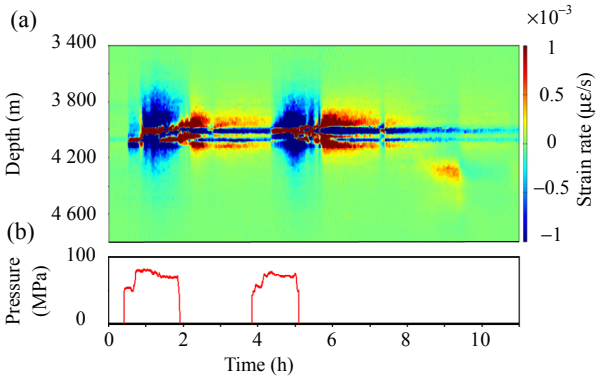

Fig. 9 Results of offset-well hydraulic fracturing monitoring: (a) stratigraphic strains picked up by the optic cable in the neighboring well during the hydraulic fracturing process and (b) casing pressure of the fracturing well.

3.5 Surface seismic exploration using the uDAS with the helical fiber-optic cable

Surface seismic exploration is a key approach for obtaining deep structural information in the oil and gas exploration and development. The conventional discrete geophone arrays suffer from insufficient spatial sampling, severe aliasing, and relatively poor repeatability. In contrast, helical fiber-optic cables enable continuous, high-density, and multi-azimuth measurement, providing repeatable surface observations to improve near-surface modeling and static correction quality, thereby enhancing the deep imaging accuracy and

4-dimensional (4D) monitoring reliability.

Surface seismic exploration using the uDAS with the helical fiber-optic cable is carried out, as shown in Fig. 10(a), providing multi-azimuth strain sensitivity and allowing the sensing fiber to respond to wavefields with different incidence directions and wave modes (e.g., P-waves and surface waves). Figure 10(b) presents the record acquired by the uDAS instrument, in which direct waves, reflections, and surface waves are clearly identifiable, indicating that the helical cable enhances the observability of multi-wave components. Furthermore, 2D imaging profiles are obtained using the reflection wave imaging technology, as shown in Fig. 10(c). The shallow interval exhibits continuous and well-resolved reflection events with the high SNR. This result demonstrates that the uDAS instruments combined with the helical fiber-optic cable can provide reliable solutions for near-surface inversions of velocity, attenuation, and anisotropy.

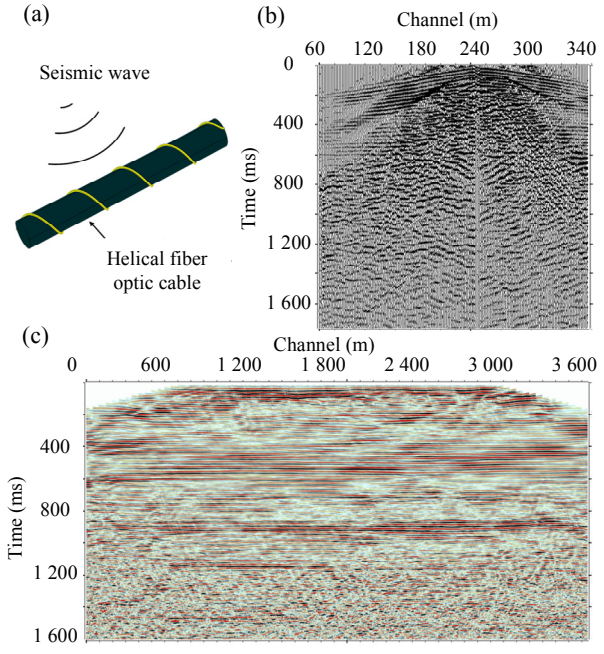

Fig. 10 Results of surface seismic exploration: (a) helical fiber-optic cable, (b) the record acquired by the uDAS instrument, and (c) 2-dimensional (2D) imaging profiles.

3.6 Near-surface structural investigation

Near-surface structural investigation is a foundational task in the oil and gas exploration and development, as it can provide accurate near-surface velocity models and static corrections for seismic data processing, removing waveform distortions introduced by near-surface heterogeneity and thereby significantly improving the accuracy and reliability of deep structural imaging. It is also essential for pre-drill engineering risk assessment and plays a critical role across multiple aspects of drilling engineering, including shallow geohazard identification, wellbore-design optimization, and safe execution of drilling operations. These contributions do help the improvement in the exploration success and the reduction in development costs. Compared with the traditional geophone arrays, the uDAS offers the sub-meter spatial sampling resolution, enabling high-density and large-scale shallow-surface imaging.

A near-surface structural investigation is conducted using a straight fiber-optic cable deployed horizontally on the ground, as shown in Fig. 11(a). Seismic waves are generated by a hammer source, and the wavefields are recorded by the uDAS. Through long-term stacking of cross-correlation functions, empirical Green's functions of surface waves are retrieved. Phase-velocity dispersion curves are then extracted and inverted to build a shear-wave (S-wave) velocity profile of the shallow subsurface, as illustrated in Fig. 11(b). The resulting velocity distribution reveals stratigraphic layering and lateral heterogeneity within the upper ~15 m, clearly delineating the morphology of shallow interfaces. The result shows that the uDAS can provide continuous and meter-scale near-surface measurement, and support accurate static corrections and more reliable deep imaging, attributing the interpretation with high-resolution near-surface velocity models.

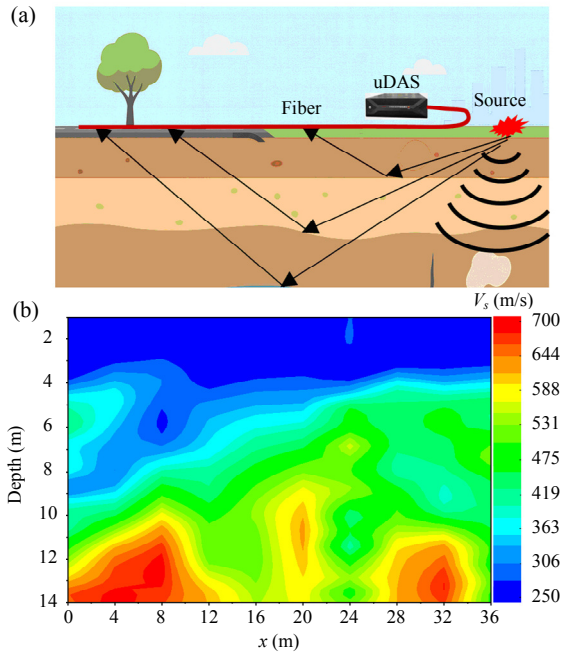

Fig. 11 Schematic diagram and results of uDAS near-surface structural investigation: (a) schematic diagram of near-surface structural investigation and (b) stratigraphic velocity profiles.

3.7 uDAS-uphole

The DAS-uphole offers a direct means of near-surface velocity measurement. First-arrival travel-time inversion yields high-precision layer velocities, resolving thin interbeds and small-scale features near the wellbore. The resulting high-resolution velocity model offers essential near-surface information for accurate imaging of mid- to deep-reservoir targets. Leveraging its sub-meter spatial sampling resolution, the uDAS continuously acquires distributed seismic data along the borehole to build the shallow velocity model adjacent to the well.

To further evaluate the applicability of the uDAS-uphole, a survey is conducted using the uDAS in a vertical well approximately 360 m deep, where a vibroseis source is employed for excitation. Figure 12(a) shows the seismic record acquired, which exhibits continuous, coherent, and high SNR first-arrival, indicating the excellent borehole coupling stability and high-fidelity measurement performance. Figure 12(b) presents the first-arrival curve, and the velocity and associated stratigraphic depth are derived from the time-depth relationship, where the velocity increases gradually from approximately 500 m/s near the surface to more than 3 300 m/s at a depth of 350 m. This variation corresponds to a stratigraphic transition from unconsolidated sediments to compacted rock layers. The near-wellbore near-surface velocity model obtained with the uDAS provides important support for deep-reservoir structural analysis and lithologic interpretation.

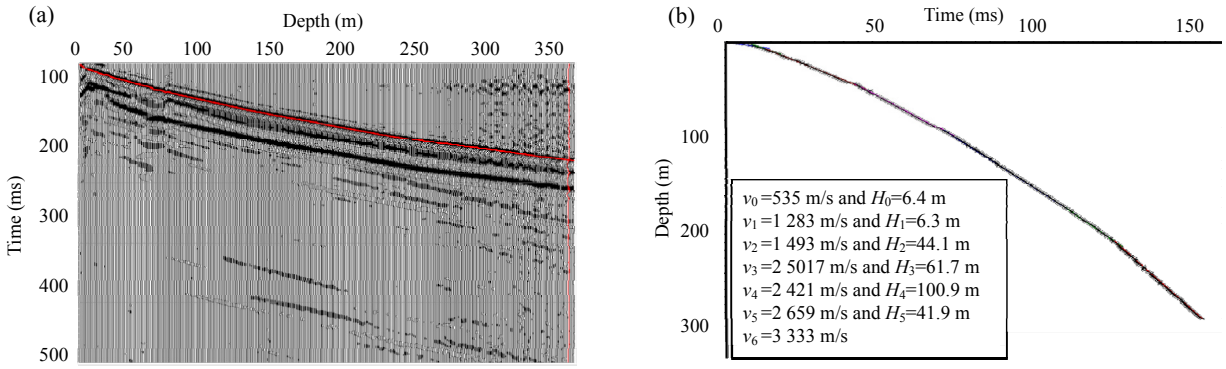

Fig. 12 Results of uDAS-uphole: (a) record acquired by the uDAS and (b) first-arrival curve.

4. Discussion

To present the characteristics of the above applications and the corresponding uDAS parameter configurations in greater detail, we have summarized them in Table 2.

To further enhance the uDAS and its applications, efforts could be focused on the following issues:

1) To achieve higher quality seismic data acquisition at the long sensing range (e.g., ultra-deep wells exceeding 6 000 m), we can integrate pulse coding schemes [45], chirped modulation method [46, 47], and scattering-enhanced fibers [48] into the uDAS system. Moreover, artificial intelligence can be incorporated into the uDAS data processing workflow for improving the signal quality.

2) Although the uDAS is presently focused on oil and gas applications, its world-class performance far exceeds typical sensing requirements for other industries. For example, it can be easily extended to integrity monitoring of the petrochemical equipment, leakage detection of oil/gas pipelines, and long-term monitoring of large-scale civil infrastructure.

Table 2 Characteristics of representative applications and the corresponding uDAS parameter configurations.

Applications	Typical characteristics	uDAS parameter configurations
VSP (onshore/offshore)	Continuous acquisition along the entire borehole for seismic waves with the dominant frequency content from a few to several hundred Hz and well depth up to several km	Full-wellbore coverage with the tunable GL of 2 m–40 m, the channel spacing of 1 m, and the bandwidth of 1 Hz–500 Hz
Single-well hydraulic fracturing monitoring	High-frequency vibration signals indicating the fluid-entry location and injected fluid volume	Effective bandwidth from tens of Hz to several kHz, enabling resolution of single-cluster fracturing responses
Offset-well hydraulic fracturing monitoring	Low-frequency formation signals reflecting fracture development and evolution	Detection of low-frequency signals down to the mHz range and accurately capturing formation deformation in the monitoring well
Surface seismic exploration and near-surface structural investigation	High-density shallow seismic data acquired with the buried fiber-optic cable, with the frequency content from a few to several hundred Hz and target depths of tens to several hundred meters	Sub-meter equivalent channel spacing and bandwidth of 1 Hz–500 Hz, supporting velocity inversion and high-resolution imaging of near-surface structures
DAS-uphole	Typical well depth of less than several hundred meters, requiring the high spatial resolution to identify fine structures	Sub-meter spatial sampling, enabling effective identification of thin geological layers

In summary, we introduce our world-class uDAS instrument with the broad application adaptability and robust engineering capability covering the major stages in the oil and gas exploration and development. For the applications mentioned above, the uDAS can provide high-fidelity signal acquisition across the entire well, enabling the accurate detection of formation responses, dynamic characterization of fracturing, and production processes, as well as high-resolution imaging of stratigraphic structures. The uDAS is replacing electronic geophone arrays as the next-generation all-optical geophones.

Acknowledgment

This work was funded by the National Natural Science Foundation of China (Grant Nos. 41527805 and 51875091); Ministry of Science and Technology of the People's Republic of China (Grant No. 2024ZD1404704); China National Petroleum Corporation (Grant No. 2023ZZ05-03); China Southern Power Grid Company Limited [Grant No. 291 funded by Qiankehe (2023)]; State Grid Corporation of China (Grant Nos. 5700-202499324A-1-3-ZB and 5500-202326527A-3-2-ZN).

Declarations

Conflict of Interest Yunjiang RAO is the editor-in-chief for Photonic Sensors and was not involved in the editorial review, or the decision to publish this article. All authors declare that there are no competing interests.

Permissions All the included figures, tables, or text passages that have already been published elsewhere have

Use of AI Statement None.

References

[1] Z. Lin, S. Duan, M. Liu, C. Dang, S. Qian, L. Zhang, *et al*., "Insights into materials, physics, and applications in flexible and wearable acoustic sensing technology," *Advanced Materials*, 2024, 36(9): e2306880.

[2] Z. Lin, G. Zhang, X. Xiao, C. Au, Y. Zhou, C. Sun, *et al*., "A personalized acoustic interface for wearable human-machine interaction," *Advanced Functional Materials*, 2021, 32(9): 2109430.

[3] X. Bao, Z. Zhou, and Y. Wang, "Review: distributed time-domain sensors based on Brillouin scattering and FWM enhanced SBS for temperature, strain and acoustic wave detection," *Photonix*, 2021, 2(1): 14.

[4] Y. Rao, Z. Wang, H. Wu, Z. Ran, and B. Han, "Recent advances in phase-sensitive optical time domain reflectometry (*Φ*-OTDR)," *Photonic Sensors*, 2021, 11(1):1–30.

[5] L. Shao, J. Zhang, X. Chen, D. Xu, H. Gu, Q. Mu, *et al*., "Artificial intelligence-driven distributed acoustic sensing technology and engineering application," *PhotoniX*, 2025, 6: 4.

[6] H. Li, C. Fan, T. Liu, Y. Liu, Z. Yan, P. Shum, *et al*., "Time-slot multiplexing based bandwidth enhancement for fiber distributed acoustic sensing," *Science China Information Sciences*, 2021, 65(1): 119303.

[7] M. Sun, M. Yu, H. Wang, K. Song, X. Guo, S. Xue, *et al*., "Intelligent water perimeter security event recognition based on NAM-MAE and distributed optic fiber acoustic sensing system," *Optics Express*, 2023, 31(22): 37058–37073.

[8] G. Yan, D. Wang, J. Long, L. Jiang, Y. Gong, Z. Ran, *et al*., "High-performance towing cable hydrophone array with an improved ultra-sensitive fiber-optic distributed acoustic sensing system," *Optics Express*, 2023, 31(16): 25545–25556.

[9] M. A. Rahman, H. Taheri, F. Dababneh, S. S. Karganroudi, and S. Arhamnamazi, "A review of distributed acoustic sensing applications for railroad condition monitoring," *Mechanical Systems and Signal Processing*, 2024, 208: 110983.

[10] M. S. Amat, D. F. Sánchez, H. F. Martins, D. V. Fontcuberta, J. Preciado-Garbayo, S. Martin-Lopez, *et al*., "Monitoring of a highly flexible aircraft model wing using time-expanded phase-sensitive OTDR," *Sensors*, 2021, 21(11): 3766.

[11] T. Yang, Y. Xiao, Z. Ran, X. He, T. Shao, W. Wang, *et al*., "Design of a weak fiber Bragg grating acoustic sensing system for pipeline leakage monitoring in a nuclear environment," *IEEE Sensors Journal*, 2021, 21(20): 22703–22711.

[12] J. Chen, H. Li, X. Xiao, C. Fan, B. Yan, S. Zhang, *et al*., "Fully distributed hydroacoustic sensing based on ultra-highly sensitive and lightweight fiber-optic hydrophone cable," *Optics and Lasers in Engineering*, 2023, 169: 107734.

[13] M. R. Fernandez-Ruiz, H. F. Martins, E. F. Williams, C. Becerril, R. Magalhaes, L. Costa, *et al*., "Seismic monitoring with distributed acoustic sensing from the near-surface to the deep oceans," *Journal of Lightwave Technology*, 2022, 40(5): 1453–1463.

[14] F. Walter, D. Gräff, F. Lindner, P. Paitz, M. Köpfli, M. Chmiel, *et al*., "Distributed acoustic sensing of microseismic sources and wave propagation in glaciated terrain," *Nature Communications*, 2020, 11(1): 2436.

[15] T. He, Q. Sun, S. Zhang, H. Li, B. Yan, C. Fan, *et al*., "A dual-stage-recognition network for distributed optical fiber sensing perimeter security system," *Journal of Lightwave Technology*, 2023, 41(13): 4331–4340.

[16] S. Yan, Y. Shang, C. Wang, W. Zhao, and J. Ni, "Mixed intrusion events recognition based on group convolutional neural networks in DAS system," *IEEE Sensors Journal*, 2022, 22(1): 678–684.

[17] L. Gan, L. Dang, D. Wang, Y. Wang, G. Chen, Q. Liu, *et al*., "Research on the processing and interpretation methods of distributed fiber optic vibration signal logging injection profiles," *Geoenergy Science and Engineering*, 2024, 239: 212980.

[18] B. Han, H. Guan, J. Yao, Y. J. Rao, Z. Ran, Y. Gong, *et al*., "Distributed acoustic sensing with sensitivity-enhanced optical cable," *IEEE Sensors Journal*, 2021, 21(4): 4644–4651.

[19] D. A. Otchere, A. H. Latiff, and B. N. Tackie-Otoo, "Distributed acoustic sensing in subsurface applications – review and potential integration with artificial intelligence for an intelligent CO_2 storage monitoring system," *Geoenergy Science and Engineering*, 2024, 237: 212818.

[20] X. Qiao, C. Wang, W. Zhao, W. Wang, X. Sui, G. Liu, *et al*., "A method for data denoising and smoothing based on DAS VSP," *IEEE Transactions on Instrumentation and Measurement*, 2025, 74: 1–8.

[21] R. Zheng, L. Fang, D. Yang, and Q. Deng, "Study on

multiphase flow in horizontal wells based on distributed acoustic sensing monitoring," *Processes*, 2025, 13(7): 2280.

[22] I. Ashry, Y. Mao, B. Wang, F. Hveding, A. Bukhamsin, T. K. Ng, *et al*., " A review of distributed fiber-optic sensing in the oil and gas industry," *Journal of Lightwave Technology*, 2022, 40(5): 1407–1431.

[23] L. Qu, W. Pan, K. Innanen, M. Macquet, and D. Lawton, "Feasibility study of anisotropic full-waveform inversion with DAS data in a vertical seismic profile configuration at the Newell County Facility, Alberta, Canada," *Surveys in Geophysics*, 2024, 45(4): 1117–1142.

[24] C. Young, J. Shragge, W. Schultz, S. Haines, C. Oren, J. Simmons, *et al*., "Advanced distributed acoustic sensing vertical seismic profile imaging of an Alaska north slope gas hydrate field," *Energy & Fuels*, 2022, 36(7): 3481–3495.

[25] Y. Zhao, Y. Li, and N. Wu, "Distributed acoustic sensing vertical seismic profile data denoiser based on convolutional neural network," *IEEE Transactions on Geoscience and Remote Sensing*, 2021, 60: 1–11.

[26] S. Gautam, C. Guria, and V. K. Rajak, "A state of the art review on the performance of high-pressure and high-temperature drilling fluids: towards understanding the structure-property relationship of drilling fluid additives," *Journal of Petroleum Science and Engineering*, 2022, 213: 110318.

[27] R. Singh, R. Sharma, and G. R. Rao, "Investigation of the effects of ultra-high pressure and temperature on the rheological properties of a novel high-density clear completion fluids using magnesium bromide for applications in HPHT reservoirs," *Geomechanics and Geophysics for Geo-Energy and Geo-Resources*, 2024, 10(1): 9.

[28] Y. Vaezi and M. van der Baan, "Interferometric assessment of clamping quality of borehole geophones," *Geophysics*, 2015, 80(6): WC89–WC98.

[29] T. Reid, G. Li, D. Zhu, and A. D. Hill, "Experimental investigation of low-frequency distributed acoustic sensor responses to two parallel propagating fractures," *Sensors (Basel)*, 2024, 24(12): 3880.

[30] J. Saw, X. Zhu, L. Luo, J. Correa, K. Soga, and J. Ajo-Franklin. "Distributed fiber optic sensing for in-well hydraulic fracture monitoring," *Geoenergy Science and Engineering*, 2025, 250: 213792.

[31] G. Naldrett, C. Cerrahoglu, and V. Mahue. "Production monitoring using next-generation distributed sensing systems," *Petrophysics – The SPWLA Journal of Formation Evaluation and Reservoir Description*, 2018, 59(4): 496–510.

[32] R. Isaenkov, R. Pevzner, S. Glubokovskikh, S. Yavuz, P. Shashkin, A. Yurikov, *et al*., "Advanced time-lapse processing of continuous DAS VSP data for plume evolution monitoring: stage 3 of the CO_2CRC Otway project case study," *International Journal of Greenhouse Gas Control*, 2022, 119: 103716.

[33] F. Su, X. Li, Y. Feng, S. Li, Y. Wang, C. Gu, *et al*., "Sophisticated distributed acoustic sensing (DAS) for real-time monitoring and analysis of wellbore integrity," *Geoenergy Science and Engineering*, 2026, 256: 214162.

[34] A. K. O. Perez and M. van der Baan, "Interpretation of low-frequency distributed acoustic sensing data based on geomechanical models," *Geophysics*, 2024, 89(2): M47–M59.

[35] A. Ellmauthaler, M. LeBlanc, J. Bush, M. E. Willis, J. L. Maida, and G. A. Wilson, "Real-time DAS VSP acquisition and processing on single- and multi-mode fibers," *IEEE Sensors Journal*, 2021, 21(13): 14847–14852.

[36] J. Sharma, T. Cuny, O. Ogunsanwo, and O. Santos, "Low-frequency distributed acoustic sensing for early gas detection in a Wellbore," *IEEE Sensors Journal*, 2021, 21(5): 6158–6169.

[37] Y. Zheng, Y. Wang, X. Liang, Q. Xue, E. Liang, S. Wu, *et al*., "A deep learning approach for signal identification in the fluid injection process during hydraulic fracturing using distributed acoustic sensing data," *Frontiers in Earth Science*, 2022, 10: 999530.

[38] W. Tegtow, N. Boitz, and S. A. Shapiro, "Integrating microseismicity and low-frequency distributed acoustic sensing to characterize hydraulic fracturing," *Geophysics*, 2025, 90(3): M75–M84.

[39] Y. Rao, Z. Ran, and K. Xie, "Methods for improving the performance of distributed sensing systems using subcarrier technology," China Patent ZL200710048376.X, Sept. 12, 2007.

[40] Y. Rao, T. Zhu, Z. Ran, Y. Wang, J. Jiang, and A. Hu, "Novel long-period fiber gratings written by high-frequency CO_2 laser pulses and applications in optical fiber communication," *Optics Communications*, 2004, 229(1–6): 209–221.

[41] Z. Ran, H. Yang, and Y. Rao, "A spectral acquisition method and its acquisition system," China patent ZL201310262570.3, Jun. 27, 2013.

[42] Silixa, Intelligent distributed acoustic sensor (iDAS™), [Online]. Available, https://silixa.com /technology/idas-intelligent-distrib uted-acoustic-sensor/, 2024.

[43] Halliburton, DataSphere® DAS interrogator, [Online]. Available, https://cdn.bfldr.com/ IQ55YUSL/as/fk75h6pt8p9nbx9c4rrxvqj/DataSpher e_DAS_interrogator_-_Data_sheet, 2025.

[44] Schlumberger, Optiq distributed acoustic sensing interrogator, [Online]. Available, https://www.slb. com/search#q=DAS&t=slbcom, 2025.

[45] P. Wang, H. Zhang, J. Chen, P. Guo, Y. Wang, X. Liu *et al.*, "Ultra-long range distributed acoustic sensor

using poly-phase coding approach," *Journal of Lightwave Technology*, 2024, 42(7): 2595–2603.
[46] J. Xiong, Z. Wang, Y. Wu, and Y. Rao. "Single-shot COTDR using sub-chirped-pulse extraction algorithm for distributed strain sensing," *Journal of Lightwave Technology*, 2020, 38(7): 2028–2036.
[47] D. Chen, Q. Liu, Y. Wang, H. Li, and Z. He. "Fiber-optic distributed acoustic sensor based on a chirped pulse and a non-matched filter," *Optics Express*, 2019, 27(20): 29415–29424.
[48] A. Masoudi, T. Lee, M. Beresna, and G. Brambilla. "10-cm spatial resolution distributed acoustic sensor based on an ultra low-loss enhanced backscattering fiber," *Optics Continuum*, 2022, 1(9): 2002–2010.